ELSEVIER

Engineering Analysis with Boundary Elements 27 (2003) 333–343

ENGINEERING ANALYSIS *with* BOUNDARY ELEMENTS

www.elsevier.com/locate/enganabound

Generalized excitations and loads for electromagnetic analysis with boundary elements

Branislav M. Notaroš[a,*], Branko D. Popović[b]

[a]*Department of Electrical and Computer Engineering, University of Massachusetts Dartmouth, 285 Old Westport Road, North Dartmouth, MA 02747-2300, USA*

[b]*Department of Electrical Engineering, University of Belgrade, P.O. Box 35-54, 11120 Belgrade, Yugoslavia*

Received 31 March 2002; accepted 25 May 2002

Abstract

Several new excitation and load models are proposed for electromagnetic analysis in the context of a Galerkin-type large-domain (higher-order) boundary element method (BEM) or Method of moments for structures composed of thin wires, metallic surfaces, and imperfect inhomogeneous dielectric bodies. The models represent a natural generalization of point-delta generators and loads for wires. They are used for excitation and loading of metallic quadrilateral surface elements and dielectric hexahedral volume elements, and are termed line-delta and surface-delta generators and loads, respectively. The corresponding Galerkin generalized impedance and voltage matrix elements are derived and incorporated in the large-domain BEM outlined in the paper. The accuracy and usefulness of the proposed excitation and load models are illustrated on a number of characteristic examples. It is believed that these models can also be included in other BEMs for analysis of electromagnetic systems in frequency domain with comparable advantages.

Keywords: Excitations; Loads; Boundary elements; Moment method; Integral equations; Electromagnetic analysis

1. Introduction

Modelling and treatment of excitations and loads is one of the most delicate, and most important, problems in numerical analysis of electromagnetic structures based on the boundary element method (BEM) or the method of moments (MoM) [1]. Even for the structures containing only thin wires, none of the several approaches for excitation and load modeling in the context of the BEM/MoM [2] cannot be said to represent an ideal solution for all geometrical and material configurations and all practical occasions. The delta-function (point) voltage generator along wires is simple, but the susceptance it yields increases with the degree of current approximation. The TEM magnetic-current frill, which originated in the approximation of the coaxial-cable excitation, does not have this deficiency. However, because of the assumption implicit in the frill generator that the system is axially symmetrical in the vicinity of the generator, it is of limited usefulness in the analysis of general three-dimensional (3D) structures, and great caution needs to be exercised whenever it is used. The coaxial-cable feed may be simplified as a thin filament of impressed current, which must be electrically very short. This simple current probe generator can replace the TEM frill generator in some applications. The fourth choice is a voltage gap generator, producing a scalar-potential jump across a gap (of finite width) between two wire segments. In fact, these four models appear to be the only ones that have been used for approximating concentrated excitations of arbitrary electromagnetic structures. Thus, in order to excite a structure by concentrated generators, it was necessary to have some wire segments, however short, although the structure itself might not have any wires at all. Another possibility is a gap generator between two narrow strips, but it is not uniquely defined, because its width, except that it should be small when compared with the wavelength, can have any value.

Similarly, for the approximation of concentrated loads mostly delta loads and short-wire segment loads appear to have been used. To simulate a concentrated load it was also

* Corresponding author. Tel.: +1-508-910-6464; fax: +1-508-999-8489.
E-mail addresses: bnotaros@umassd.edu (B.M. Notaroš), ebdp@etf.bg.ac.yu (B.D. Popović).

0955-7997/02/$ - see front matter © 2002 Elsevier Science Ltd. All rights reserved.
PII: S0955-7997(02)00121-2

necessary to have at least a short wire segment, although the structure may not have wires at all.

This paper proposes several new excitation and load models that represent a natural generalization of the delta excitations and loads for wires. The new excitation and load models are used with infinitely thin metallic plates and (imperfect) dielectric bodies. For plates, two sides of a common edge of two joined conducting surfaces are assumed to be at different potentials, i.e. that across the edge there is a scalar-potential jump (the same along the edge). This jump may be due to fictitious generators distributed along this line, and acting normally to it. Such a distributed generator can appropriately be named the *line-delta generator*. Alternatively, the scalar-potential jump may be due to a voltage drop across a fictitious or actual load in the form of a line (e.g. the load between the two strip segments of a printed antenna or circuit), where the voltage drop is produced by the current component normal to the line. We term such a load the *line-delta load*. Physically, line-delta generators should be short when compared with the wavelength. This restriction does not apply to line-delta loads.

For two (imperfect and inhomogeneous) dielectric bodies in contact over a common side, we similarly assume a scalar-potential jump through this surface (the same over the entire surface). In the excitation case, we attribute this jump to generators distributed over the surface and acting normally to it at all points. Such a generator we term the *surface-delta generator*. In the load case, we assume that there is a distributed load over the surface such that a current normal to it produces a scalar-potential jump across it. We term such a load the *surface-delta load*. Physically, the extent of the surface-delta generators in any direction needs to be much smaller than the wavelength, while such a restriction does not apply to surface-delta loads.

It will be shown that these simple types of generators and loads are very useful in the BEM analysis of 3D electromagnetic structures. As a simple example, an antenna in the form of two thin metallic sheets does not need any more a short wire segment with a generator between them, requiring wire-to-plate junctions with all associated problems. Instead, a line-delta generator can be assumed between a narrow edge common to the two plates. As another example, an antenna made of an imperfect dielectric can be driven directly by a surface-delta generator; the excitation of such an antenna with classical excitations along wires is not only much more difficult to model, but also very sensitive to the model size and shape.

The novel types of excitations and loadings can, in principle, be used with any type of numerical solution based on the integral-equation formulation in frequency domain. In this paper, the algorithms for their inclusion in the numerical model are derived in detail for a Galerkin-type large-domain (higher-order) BEM (MoM) for analysis of general 3D electromagnetic structures, composed of thin wires, metallic surfaces, and dielectric bodies. In the method, the wires are modeled by straight-wire segments [3], surfaces by bilinear quadrilaterals [4], and volume elements by trilinear hexahedrons [5]. Approximate current distributions in all elements are adopted to be high-degree polynomials (in one, two or three dimensions) [3–5], which make possible for the elements to be of large electrical size. The method, consequently, belongs to the group of higher-order or large-domain (often referred to as entire-domain) methods [3–7]. Although relatively specific, the authors believe that the derivations can be of significant help in introducing the proposed excitations and loadings in other BEM/MoM techniques, and even in techniques not aimed at solving integral equations (e.g. in the finite element methods [8]).

Section 2 of the paper reviews the excitation and load models for wires, whereas Sections 3 and 4 describe the new proposed excitation and load models for surfaces and bodies, respectively, all in the context of the large-domain BEM. Given in Section 5 are the numerical examples illustrating the usefulness of the new types of excitation and load and showing good stability of the results. It is also shown that very good agreement of the results is obtained with approximately equivalent excitations, as well as with approximately equivalent loads, of different types.

2. Brief overview of excitation and load models for wires

Since the proposed extensions of excitations and loads lean heavily on those for wires, we first review briefly basic concepts connected with wires in a large-domain BEM solution for current distribution along wires.

Consider an arbitrary wire structure situated in a time-harmonic incident (impressed) field of complex electric field intensity $\mathbf{E}_\mathrm{i}$ and angular frequency ω. This field induces line currents, of intensity I, along the generatrices of wires, l_wires (the reduced-kernel approximation for wires). The induced currents, considered in free-space, are the sources of the scattered field

$$\mathbf{E}_\mathrm{s} = -\mathrm{j}\omega\mu_0 \int_{l_\mathrm{wires}} \left(I\mathbf{l}_0 + \frac{1}{\beta_0^2}\frac{\mathrm{d}I}{\mathrm{d}l}\,\mathrm{grad} \right) g \,\mathrm{d}l, \tag{1}$$

where $\mathbf{l}_0$ is the unit vector along the wire. The free-space Green's function, g, is given by

$$g = \frac{e^{-\mathrm{j}\beta_0 R}}{4\pi R}, \qquad \beta_0 = \omega\sqrt{\varepsilon_0\mu_0}, \tag{2}$$

with R being the distance of the field point from the source point and β_0 the free-space phase coefficient. On wire surfaces, the locally longitudinal tangential component of the total electric field vector, $\mathbf{E}_\mathrm{total} = \mathbf{E}_\mathrm{i} + \mathbf{E}_\mathrm{s}$, is zero. By the theorem on extended boundary conditions [9], this request can be transferred to the wire axis, resulting in

$$-(E_\mathrm{s})_\mathrm{axial} = (E_\mathrm{i})_\mathrm{axial} \qquad \text{(along wires)}. \tag{3}$$

Eq. (3), which includes Eqs. (1) and (2), represents an electric-field integral equation (EFIE) for current distribution I along wires.

2.1. Geometrical model and current approximation for wires

The building-block for approximating wires in our large-domain BEM/MoM technique is a straight-wire segment, Fig. 1. The parametric equation of the segment axis is

$$\mathbf{r}(u) = r_0 + r_u u, \qquad 0 \le u \le 1. \tag{4}$$

In this equation, $\mathbf{r}(u)$ is the position vector of a point on the segment axis with the local coordinate u, $\mathbf{r}_0$ the position vector of the segment starting point, **O**, and $\mathbf{r}_u$ a constant vector representing the difference between the position vector of the segment end point, A, and $\mathbf{r}_0$. Let us also introduce the length coordinate x defined by the relation $x = x_1 u$, where x_1 represents the actual length of the segment (Fig. 1).

We approximate the current I along the segment by a large-domain series of polynomial basis functions with unknown coefficients. The basis functions are in the following form:

$$I_i^{(b)}(u) = P_i(u) = \begin{cases} u^i - u, & i \neq 1 \\ u, & i = 1 \end{cases}, \qquad 0 \le u \le 1, \tag{5}$$

$$i = 0, 1, \ldots, N_u,$$

where N_u is the order of approximation. Note that of all the adopted basis functions only u and $(1-u)$ are nonzero at one of the segment ends (these are, in fact, 1D rooftop functions). They are used to satisfy the boundary conditions (Kirchhoff's current law) at the segment ends. All the other basis functions are zero at the segment ends, and are used to improve the approximation of current along the segment (Fig. 2). The unknown coefficients are obtained by MoM. If we use the Galerkin type of the method of moments [1], the testing (weighting) functions are the same as the basis functions, $I_i^{(t)}(u) = I_i^{(b)}(u)$. Note that N_u can be large, which allows the current to be approximated accurately along segments as long as few wavelengths (large-domain method).

Eq. (3), applied to the wire segment in Fig. 1, becomes

$$-E_{su}(u) = E_{iu}(u), \qquad 0 \le u \le 1, \tag{6}$$

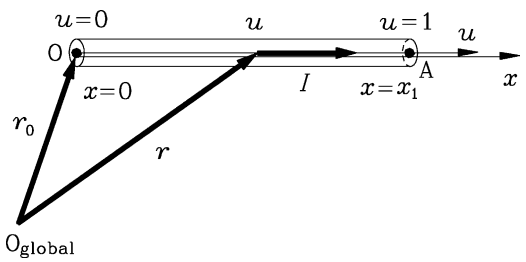

Fig. 1. Straight wire segment.

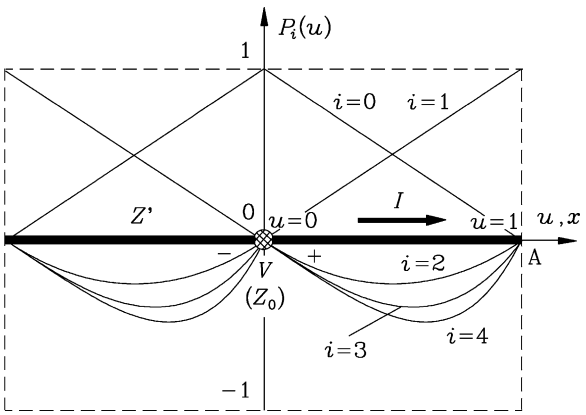

Fig. 2. Two interconnected wire segments with polynomial basis/testing functions.

where E_{iu} and E_{su} are the longitudinal components (u-components) of the impressed and scattered field, respectively, along the segment axis. The corresponding method-of-moments equation is

$$[\mathscr{Z}][a] = [\mathscr{U}], \tag{7}$$

where the matrices $[\mathscr{Z}]$ and $[\mathscr{U}]$ are known as the matrix of generalized impedances and that of generalized voltages, respectively. The matrix $[a]$ contains the unknown current-distribution coefficients (unknowns of the problem).

2.2. Excitation of wires

Generally, all excitations can be considered as distributed. For an electric field having an $E_{iu}(u)$ axial component, the Galerkin generalized voltages are evaluated as

$$U_i = \int_{u=0}^{1} I_i^{(t)}(u) E_{iu}(u) \mathrm{d}x = x_1 \int_{u-0}^{1} P_i(u) E_{iu}(u) \mathrm{d}u, \tag{8}$$

$$i = 0, 1, \ldots, N_u.$$

Two most commonly used excitations of wires are the TEM magnetic-current frill and the delta-function voltage generator. The first approximates the coaxial-line excitation. If the frill is centered at the origin of a local cylindrical $(\rho - \phi - z)$ coordinate system with the frill axis along the z-axis, the impressed electric field is of the form [2]

$$\mathbf{E}_i(\rho, \phi, z) = -\frac{4V}{\ln(b/a)} \left[z \int_a^b \int_0^{\pi} \frac{\cos\psi}{R} \frac{\mathrm{d}g(R)}{\mathrm{d}R} \mathrm{d}\psi \, \mathrm{d}r \mathbf{i}_\rho(\phi) + \int_0^{\pi} g(R)|_{r=a}^{r=b} \mathrm{d}\psi \mathbf{i}_z \right], \tag{9}$$

$$R = \sqrt{\rho^2 + z^2 + r^2 - 2\rho r \cos\psi}.$$

In this expression, g is the Green's function given by Eq. (2), V is the voltage at the coaxial line opening, and a and b are the inner and the outer radius of the cable (and of the frill). It is assumed that $b - a$ is small in terms of the wavelength, so that the TEM mode at the opening is dominant. The Galerkin

generalized voltages are obtained by introducing this expression into Eq. (8).

The TEM magnetic-current frill excitation is sometimes used as excitation of wires generally, by defining arbitrarily its parameters. Note, however, that the frill is axially symmetrical, so that excitation of a segment that is not coaxial with the frill is questionable. For example, consider a simple *V*-dipole antenna. Let the angle between the dipole arms be any angle less than 90°. Meaningless results are obtained with the TEM frill if its axis is directed along one of the two arms. Only if it is positioned symmetrically with respect to them (which in this case is perhaps logical to do), do the results agree well with those obtained by the point-delta generator excitation. However, if there are more than two wires at a junction, e.g. forming an inverted umbrella with the angle less than 90° between the wires, and one wire is excited at the junction by a TEM frill, it is virtually impossible to estimate in advance whether the results will be reliable, or not. Many other examples could be found in which the results obtained by a TEM frill are unpredictable, and frequently meaningless. As a conclusion, the TEM magnetic-current frill excitation should be used with extreme care.

A delta generator is simply a jump in the electric scalar potential across a junction of two wires. We shall term this kind of excitation the point-delta generator (instead of the usual term 'point generator'). Referring to Fig. 2, let the point-delta generator be at the point **O**, at the starting point of the segment OA. Then

$$E_{iu}(u) = V\delta(x), \tag{10}$$

where V is the generator electromotive force, and $\delta(x)$ Dirac's delta-function. When we substitute this into Eq. (8), for the Galerkin generalized voltages we obtain

$$U_i = VP_i(0)\int_{u=0}^{1}\delta(x)\mathrm{d}x = \begin{cases} V, & i=0 \\ 0, & i\neq 0 \end{cases}, \tag{11}$$

$i = 0, 1, \ldots, N_u$,

since [see Eq. (5)] $P_0(0) = 1$, and $P_i(0) = 0$ for $i > 0$.

2.3. Loads along wires

The most general load along wires is a continuous distributed load. Let per unit length it be given by $Z'(u)$. The electric field necessary to maintain the current along such a loaded wire can be represented as a compensating field

$$E_{cu}(u) = -Z'(u)I(u), \tag{12}$$

which we introduce into Eq. (8). According to Eq. (7), this results in the following additions to the Galerkin generalized impedances:

$$\begin{aligned}\Delta\mathscr{Z}_{ii'} &= -\int_{u=0}^{1} I_i^{(\mathrm{t})}(u)E_{cu}(u)\mathrm{d}x \\ &= \int_{u=0}^{1} Z'(u)I_i^{(\mathrm{t})}(u)I_{i'}^{(\mathrm{b})}(u)\mathrm{d}x \\ &= x_1\int_{u=0}^{1} Z'(u)P_i(u)P_{i'}(u)\mathrm{d}u,\end{aligned} \tag{13}$$

$i, i' = 0, 1, \ldots, N_u$.

Let now at point **O** in Fig. 2 be a concentrated (point-like) load of impedance Z_0. The voltage across the load can be replaced by a compensating generator of electromotive force

$$V_c = -Z_0 I(0), \tag{14}$$

with the reference direction indicated in Fig. 2. The corresponding compensating electric field is given by

$$E_{cu}(u) = -Z_0 I(0)\delta(x). \tag{15}$$

It results in the following addition to the Galerkin generalized impedances:

$$\Delta\mathscr{Z}_{ii} = Z_0 P_i^2(0) = \begin{cases} Z_0, & i=0 \\ 0, & i\neq 0 \end{cases}, \qquad i = 0, 1, \ldots, N_u. \tag{16}$$

We shall term such loads the point-delta loads.

3. Excitation and load models for plates

In the case of an electromagnetic structure composed of metallic surfaces (plates), the scattered field is produced by induced surface currents, of density $\mathbf{J}_s$, over the structure surface, S_{plates}. Eq. (1) thus becomes

$$\mathbf{E}_s = -j\omega\mu_0\int\int_{S_{\mathrm{plates}}}\left(\mathbf{J}_s + \frac{1}{\beta_0^2}\mathrm{div}_s\mathbf{J}_s\mathrm{grad}\right)g\ \mathrm{d}S. \tag{17}$$

The corresponding EFIE for the surface current density $\mathbf{J}_s$ over plates is obtained by stipulating that the tangential component of the total electric field at the plate surface be zero, which yields

$$-(E_s)_{\mathrm{tangential}} = (E_i)_{\mathrm{tangential}} \qquad \text{(over plates)}. \tag{18}$$

3.1. Geometrical model and current approximation for plates

In a large-domain BEM/MoM approach, it appears to be extremely convenient to approximate metallic surfaces by a system of parametric bilinear quadrilateral subsurfaces [4,7], Fig. 3. Such a quadrilateral is uniquely defined by its four vertices, which can be practically arbitrarily positioned in space. Its surface is curved, but its edges and all parametric lines are straight. In the u–v parametric

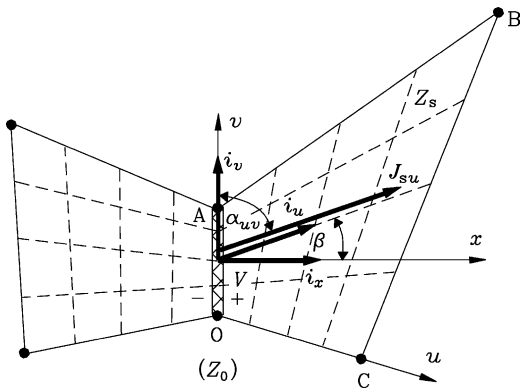

Fig. 3. Two bilinear quadrilaterals with common edge.

coordinate system in Fig. 3 it is defined by

$$\mathbf{r}(u,v) = \mathbf{r}_0 + \mathbf{r}_u u + \mathbf{r}_v v + \mathbf{r}_{uv} uv, \qquad 0 \le u, v \le 1. \tag{19}$$

In this definition, $\mathbf{r}(u, v)$ is the global position vector of a quadrilateral point with local coordinates u and v, $\mathbf{r}_0$ is the position vector of the local coordinate origin, O, and $\mathbf{r}_u$, $\mathbf{r}_v$, and $\mathbf{r}_{uv}$ are constant vectors which can be expressed easily in terms of $\mathbf{r}_0$ and the position vectors of the other three quadrilateral vertices.

The current density vector over bilinear quadrilaterals is conveniently represented by two local components as

$$\mathbf{J}_s(u,v) = J_{su}(u,v)\mathbf{i}_u(v) + J_{sv}(u,v)\mathbf{i}_v(u). \tag{20}$$

The local base unit vectors are given by

$$\mathbf{i}_u(v) = \frac{1}{e_u(v)}\frac{\partial \mathbf{r}(u,v)}{\partial u}, \qquad \mathbf{i}_v(u) = \frac{1}{e_v(u)}\frac{\partial \mathbf{r}(u,v)}{\partial v}, \tag{21}$$

where $e_u ie_v$ are the Lamé coefficients,

$$e_u(v) = \left|\frac{\partial \mathbf{r}(u,v)}{\partial u}\right|, \qquad e_v(u) = \left|\frac{\partial \mathbf{r}(u,v)}{\partial v}\right|. \tag{22}$$

We adopt the following higher-order basis and test functions for the u-component of the surface current density vector [4,7]:

$$\mathbf{J}^{(b)}_{suij}(u,v) = \mathbf{J}^{(t)}_{suij}(u,v) = \frac{1}{e_v(u)\sin\alpha_{uv}(u,v)} P_i(u) Q_j(v) \mathbf{i}_u(v), \tag{23}$$

$$0 \le u, v \le 1, \qquad i = 0, 1, \ldots, N_u, \qquad j = 0, 1, \ldots, N_v,$$

where $P_i(u)$ is defined in Eq. (5), and

$$Q_j(v) = v^j, \qquad j = 0, 1, \ldots, N_v. \tag{24}$$

N_u and N_v are the orders of approximation, and $\alpha_{uv}(u, v)$ is the angle between the u and v coordinate line at (u, v). The v-component of $\mathbf{J}_s$ is represented in analogous manner. In analogy with wires, these basis functions are used to impose the continuity boundary conditions along quadrilateral edges shared with other quadrilaterals, and along free quadrilateral edges, of the normal component of vector $\mathbf{J}_s$.

Contained in the expressions of the Galerkin generalized impedances for bilinear quadrilaterals, we need its area element,

$$\mathrm{d}S_{uv}(u,v) = \mathrm{d}l_u(v)\mathrm{d}l_v(u)\sin\alpha_{uv}(u,v), \tag{25}$$

where the line elements along the coordinate lines are given by

$$\mathrm{d}l_u(v) = e_u(v)\mathrm{d}u, \qquad \mathrm{d}l_v(u) = e_v(u)\mathrm{d}v. \tag{26}$$

3.2. Excitation of conducting surfaces

The most general excitation of a conducting surface is that distributed arbitrarily over it. The Galerkin generalized voltages for such an excitation are

$$U_{ij} = \int_{u=0}^{1}\int_{v=0}^{1} \mathbf{J}^{(t)}_{suij}(u,v)\cdot\mathbf{E}_i(u,v)\mathrm{d}S_{uv}(u,v) = \int_{u=0}^{1}\int_{v=0}^{1} P_i(u)Q_j(v)\frac{\partial \mathbf{r}(u,v)}{\partial u}\cdot\mathbf{E}_i(u,v)\mathrm{d}u\,\mathrm{d}v, \tag{27}$$

$$i = 0, 1, \ldots, N_u, \qquad j = 0, 1, \ldots, N_v.$$

Note that, in the Galerkin method, we have an analogous expression for testing by the v-component of the current density vector, $\mathbf{J}^{(t)}_{svij}(u,v)$.

This excitation model is appropriate in the analysis of metallic scatterers, but not for antennas, where wire segments with generators have to be added to the structure, although it might not have it at all. The problems associated with wire-to-surface junctions are well known. To avoid this, we introduce generators acting along common edges of two or more conducting surfaces. Such distributed generators are assumed to produce a scalar-potential jump along the common edge. Although it can be made variable along the edge, this seems to be of purely academic interest, and we consider only the case of scalar-potential jump constant along the edge. Being extensions to point-delta generators for wires, it seems appropriate to term such generators the *line-delta generators*.

Let a line-delta generator be associated with the edge OA of the bilinear quadrilateral OABC in Fig. 3. Let the quadrilateral be planar, which simplifies the derivations greatly, and does not impair the practical usefulness of the generator, since it is restricted to the very edge shared by the (possibly curved) quadrilaterals. The compensating impressed electric field resulting in the potential difference V across the common edge, with respect to the reference direction in Fig. 3, is

$$\mathbf{E}_i(u,v) = V\delta(x)\mathbf{i}_x, \tag{28}$$

where the x-axis is normal to the line generator, and is in the plane of the quadrilateral OABC. Introducing this into Eq. (27) yields the following expression for the Galerkin

generalized voltages:

$$U_{ij} = \int_{u=0}^{1}\int_{v=0}^{1} J^{(t)}_{suij}(u,v)\mathbf{E}_i(u,v)\mathbf{i}_u(v)\cdot\mathbf{i}_x \mathrm{d}S_{uv}(u,v)$$
$$= VP_i(0)\int_{u=0}^{1}\delta(x)\,\mathrm{d}x\int_{v=0}^{1} Q_j(v)\mathrm{d}v$$
$$= \begin{cases} V/(j+1), & i=0 \\ 0, & i\neq 0 \end{cases}, \qquad (29)$$
$$i=0,1,\ldots,N_u, \qquad j=0,1,\ldots,N_v.$$

where the following geometrical relations were used (see Fig. 3):

$$\mathbf{i}_u(v)\cdot\mathbf{i}_x = \cos\beta(u,v), \qquad \mathrm{d}l_u(v)\cos\beta(u,v) = \mathrm{d}x, \qquad (30)$$
$$\cos\beta(u,v) = \sin\alpha_{uv}(u,v).$$

Note that the generalized voltages relating to the v-component of the test functions are zero, since $\mathbf{i}_v(0)\cdot\mathbf{i}_x = 0$.

3.3. Loads over conducting surfaces

The most general type of loading over a conducting surface is a load distributed over the surface in arbitrary manner. Let the surface impedance over the surface be $Z_s(u,v)$ (Ω/square). It can be introduced into the equations by considering the field driving the current over the surface as a compensating impressed electric field

$$\mathbf{E}_c(u,v) = -Z_s(u,v)\mathbf{J}_s(u,v). \qquad (31)$$

According to Eqs. (27) and (7), this results in the following additions to the Galerkin generalized impedances relating to the u-component of a test function and the u-component of a basis function:

$$\Delta\mathscr{Z}_{iji'j'} = -\int_{u=0}^{1}\int_{v=0}^{1}\mathbf{J}^{(t)}_{suij}(u,v)\cdot\mathbf{E}_c(u,v)\mathrm{d}S_{uv}(u,v)$$
$$= \int_{u=0}^{1}\int_{v=0}^{1} Z_s(u,v)\cdot\mathbf{J}^{(t)}_{suij}(u,v)\cdot\mathbf{J}^{(b)}_{sui'j'}(u,v)\mathrm{d}S_{uv}(u,v)$$
$$= \int_{u=0}^{1}\int_{v=0}^{1} Z_s(u,v)P_i(u)Q_j(v)P_{i'}(u)Q_{j'}(v)$$
$$\times\frac{e_u(v)}{e_v(u)\sin\alpha_{uv}(u,v)}\mathrm{d}u\,\mathrm{d}v,$$
$$i,i'=0,1,\ldots,N_u, \qquad j,j'=0,1,\ldots,N_v. \qquad (32)$$

Similar expressions are obtained for combinations of the test and basis function u–v and v–v (a combination v–u results in the same expression as u–v).

A load over a surface analogous to the point-delta load can be introduced by assuming the distributed load to exist only along a very narrow strip near a quadrilateral edge. In the limit of infinitely narrow strip with finite impedance across the strip we thus obtain a *line-delta load*. Assume a line-delta load Z_0 to exist along the edge OA in Fig. 3. The electromotive force of the corresponding compensating line-delta generator is now not constant along the load line, since surface current density is not generally constant along it. The compensating impressed electric field across the line-delta load is given by

$$\mathbf{E}_c(u,v) = -Z_0 l_v(u)J^{(b)}_{suij}(u,v)\delta(x)\mathbf{i}_x, \qquad (33)$$

where $l_v(u)$ is the length of the part of v parametric line which belongs to the quadrilateral [$l_v(0)$ is the length of the quadrilateral edge OA]. This results in the following additions to the impedance matrix:

$$\Delta\mathscr{Z}_{ijij} = \begin{cases} Z_0/(2j+1), & i=0 \\ 0, & i\neq 0 \end{cases}, \qquad i=0,1,\ldots,N_u, \qquad (34)$$
$$j=0,1,\ldots,N_v.$$

4. Excitation and load models for bodies

Consider an electromagnetic structure composed of volume dielectric bodies with losses and excited by a field $\mathbf{E}_i$. The density of the total (polarization plus conduction) induced volume current, $\mathbf{J}$, inside the volume of the structure, V_{bodies}, is given by the generalized local Ohm's law

$$\mathbf{J} = \sigma_e\mathbf{E}_{\text{total}}, \qquad \sigma_e = \sigma + \mathrm{j}\omega(\varepsilon - \varepsilon_0), \qquad (35)$$

where σ, ε and σ_e are the conductivity, permittivity, and equivalent conductivity of the material, respectively. Using the same Green's function as in Eq. (2), the scattered field is expressed as

$$\mathbf{E}_s = -j\omega\mu_0\int\int\int_{V_{\text{bodies}}}\left(\mathbf{J} + \frac{1}{\beta_0^2}\operatorname{div}\mathbf{J}\operatorname{grad}\right)g\,\mathrm{d}V, \qquad (36)$$

and hence the EFIE for the current density $\mathbf{J}$ inside dielectric bodies

$$-\mathbf{E}_s + \frac{\mathbf{J}}{\sigma_e} = \mathbf{E}_i \qquad \text{(inside bodies)}. \qquad (37)$$

4.1. Geometrical model and current approximation for bodies

In analogy with conducting surfaces, we model imperfect-dielectric bodies by parametric volumes in the form of trilinear hexahedrons [5–7], Fig. 4. A trilinear hexahedron is defined uniquely by its eight vertices, that can be almost arbitrarily positioned in space. Its edges, and all coordinate lines, are straight, and its sides are bilinear quadrilaterals. It is defined by the following parametric equation:

$$\mathbf{r}(u,v,w) = \mathbf{r}_0 + \mathbf{r}_u u + \mathbf{r}_v v + \mathbf{r}_w w + \mathbf{r}_{uv}uv + \mathbf{r}_{uw}uw + \mathbf{r}_{vw}vw + \mathbf{r}_{uvw}uvw, \qquad 0\le u,v,w\le 1. \qquad (38)$$

Concerning the unknown quantity to be approximated and determined in the MoM, it is numerically much more convenient to substitute $\mathbf{J}$ as the unknown in Eqs. (36) and

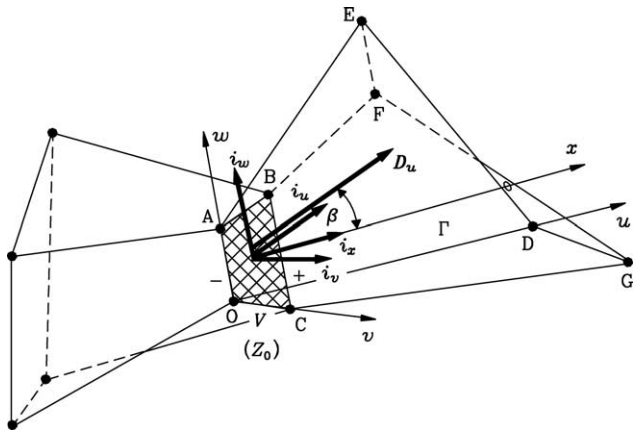

Fig. 4. Two trilinear hexahedrons with common side.

(37) by the equivalent electric displacement vector, **D**, the normal component of which is continuous at all surfaces of discontinuity in dielectric parameters inside the dielectric. This vector is related with the total electric field and with the current density in the dielectric as follows:

$$\mathbf{D} = \varepsilon_{\mathrm{e}}\mathbf{E}_{\mathrm{total}}, \qquad \varepsilon_{\mathrm{e}} = \varepsilon - \mathrm{j}\frac{\sigma}{\omega}, \qquad \mathbf{J} = \mathrm{j}\omega K\mathbf{D},$$
$$K = \frac{\varepsilon_{\mathrm{e}} - \varepsilon_0}{\varepsilon_{\mathrm{e}}}. \tag{39}$$

In these relationships, ε_{e} and K are the equivalent permittivity and electric contrast of the dielectric, respectively. The vector **D** is represented in a trilinear hexahedron by its three local components,

$$\mathbf{D}(u,v,w) = D_u(u,v,w)\mathbf{i}_u(v,w) + D_v(u,v,w)\mathbf{i}_v(u,w) + D_w(u,v,w)\mathbf{i}_w(u,v), \tag{40}$$

where the local base unit vectors and the Lamé coefficients are obtained in a manner similar to that for bilinear quadrilaterals. It appears that it is very suitable to adopt the following basis and testing functions in this case [5]:

$$\mathbf{D}^{(\mathrm{b})}_{uijk}(u,v,w) = \mathbf{D}^{(\mathrm{t})}_{uijk}(u,v,w) = \frac{1}{e_v(u,w)e_w(u,v)\sin\alpha_{vw}(u,v,w)\sin\alpha_{u(vw)}(u,v,w)} \times P_i(u)Q_j(v)Q_k(w)\mathbf{i}_u(v,w), \tag{41}$$

$0 \le u,v,w \le 1, \qquad i = 0,1,\ldots,N_u,$

$j = 0,1,\ldots,N_v, \qquad k = 0,1,\ldots,N_w.$

The angle $\alpha_{u(vw)}(u,v,w)$ is that between the u coordinate line and the v–w coordinate surface. We use these basis function to satisfy the boundary condition for the continuity of the normal component of vector **D** over a bilinear quadrilateral shared by two hexahedrons. The expression for the components D_v and D_w are analogous.

The volume differential element of a trilinear hexahedron is given by

$$\mathrm{d}V_{uvw}(u,v,w) = e_u(v,w)e_v(u,w)e_w(u,v)\mathbf{i}_u(v,w)\cdot[\mathbf{i}_v(u,w) \times \mathbf{i}_w(u,v)]\mathrm{d}u\,\mathrm{d}v\,\mathrm{d}w = e_u(v,w)e_v(u,w)e_w(u,v)\sin\alpha_{vw}(u,v,w) \times \sin\alpha_{u(v,w)}(u,v,w)\mathrm{d}u\,\mathrm{d}v\,\mathrm{d}w. \tag{42}$$

4.2. Excitation of bodies

The most general type of excitation of bodies is that distributed over its entire volume. The Galerkin generalized voltages related to the u-component of the test function in this case is

$$U_{ijk} = \int_{u=0}^{1}\int_{v=0}^{1}\int_{w=0}^{1}\mathbf{D}^{(\mathrm{t})}_{uijk}(u,v,w)\cdot\mathbf{E}_{\mathrm{i}}(u,v,w)\,\mathrm{d}V_{uvw}(u,v,w) = \int_{u=0}^{1}\int_{v=0}^{1}\int_{w=0}^{1}P_i(u)Q_j(v)Q_k(w)\frac{\partial\mathbf{r}(u,v,w)}{\partial u}\cdot\mathbf{E}_{\mathrm{i}}(u,v,w)\mathrm{d}u\,\mathrm{d}v\,\mathrm{d}w, \tag{43}$$

$i = 0,1,\ldots,N_u, \qquad j = 0,1,\ldots,N_v,$

$k = 0,1,\ldots,N_w.$

If we assume the excitation to exist in a very thin volume near a hexahedron side, in the limit when this thickness becomes vanishingly small, but the difference of the scalar-potential across the hexahedron side, normal to it, remains finite, we obtain an excitation analogous to the point-delta and line-delta generators. We term such an excitation the *surface-delta generator*. Of practical importance are only surface-delta generators with constant voltage over the entire bilinear quadrilateral, and we consider this case only.

Let the side OABC of the hexahedron OABCDEFG in Fig. 4 contain a surface-delta generator. To simplify derivations, let us assume that this hexahedron side is planar, and the x-axis be normal to it. We replace the generator by an impressed electric field as in Eq. (28), where the generator electromotive force, V, has the reference direction as in Fig. 4. The corresponding Galerkin generalized voltages for the u-component of the test functions are

$$U_{ijk} = VP_i(0)\int_{u=0}^{1}\delta(x)\mathrm{d}x\int_{v=0}^{1}Q_j(v)\mathrm{d}v\int_{w=0}^{1}Q_k(w)\mathrm{d}w = \begin{cases} V/[(j+1)(k+1)], & i = 0 \\ 0, & i \ne 0 \end{cases}, \tag{44}$$

$i = 0,1,\ldots,N_u, \qquad j = 0,1,\ldots,N_v,$

$k = 0,1,\ldots,N_w.$

This expression is obtained in a manner similar to that in obtaining Eq. (29), noting that in this case (Fig. 4)

$$\cos\beta(u,v,w) = \sin\alpha_{u(vw)}(u,v,w). \tag{45}$$

The voltages corresponding to v- and w-components of the test functions are zero, since $\mathbf{i}_v(0,w)\cdot\mathbf{i}_x = 0$ and $\mathbf{i}_w(0,v)\cdot\mathbf{i}_x = 0$.

4.3. Loads inside bodies

Since there is always an electric field at all points of a volume element, it can be visualized as a load distributed throughout the volume. We again introduce a compensating impressed electric field

$$\begin{aligned}\mathbf{E}_c(u,v,w) &= -\Gamma(u,v,w)\mathbf{D}(u,v,w),\\ \Gamma(u,v,w) &= \frac{1}{\varepsilon_e(u,v,w)},\end{aligned} \tag{46}$$

where $\Gamma(u,v,w)$ may be termed the equivalent elastance of the material. As a result, we have the following corrections of the Galerkin generalized impedances for the u-component of the test functions and the u-component of the basis functions:

$$\begin{aligned}\Delta\mathscr{Z}_{ijki'j'k'} &= -\int_{u=0}^{1}\int_{v=0}^{1}\int_{w=0}^{1}\mathbf{D}^{(t)}_{uijk}(u,v,w)\cdot\mathbf{E}_c(u,v,w)\\ &\quad\times dV_{uvw}(u,v,w)\\ &= \int_{u=0}^{1}\int_{v=0}^{1}\int_{w=0}^{1}\Gamma(u,v,w)P_i(u)Q_j(v)Q_k(w)P_{i'}(u)\\ &\quad\times Q_{j'}(v)Q_{k'}(w)\\ &\quad\times\frac{e_u(v,w)}{e_v(u,w)e_w(u,v)\sin\alpha_{vw}(u,v,w)\sin\alpha_{u(v,w)}(u,v,w)}\\ &\quad\times du\,dv\,dw,\\ i,i' &= 0,1,\ldots,N_u,\quad j,j' = 0,1,\ldots,N_v,\quad k,k' = 0,1,\ldots,N_w.\end{aligned} \tag{47}$$

We can superimpose to this volume load a load concentrated near a hexahedron side, in analogy with point-delta and line-delta loads. We shall term such a load the *surface-delta load*. Assume that such a load, Z_0, exists over the hexahedron side OABC (Fig. 4). The compensating impressed electric field is

$$\mathbf{E}_c(u,v,w) = -j\omega Z_0 S_{vw}(u)K(u,v,w)D^{(b)}_{uijk}(u,v,w)\delta(x)\mathbf{i}_x, \tag{48}$$

where $S_{vw}(u)$ is the area of the part of v–w parametric surface which belongs to the hexahedron [$S_{vw}(0)$ is the area of the hexahedron side OABC]. Note that this field is not constant over the loaded surface, since current density is not generally constant. The corresponding addition to the Galerkin impedance matrix is

$$\begin{aligned}\Delta\mathscr{Z}_{0jk0jk} &= j\omega Z_0 S_{vw}(0)\int_{v=0}^{1}\int_{w=0}^{1}\\ &\quad\times\frac{v^{2j}w^{2k}K(0,v,w)}{e_v(0,w)e_w(0,v)\sin\alpha_{vw}(0,v,w)}dv\,dw,\\ j &= 0,1,\ldots,N_v,\quad k = 0,1,\ldots,N_w\end{aligned} \tag{49}$$

$(\Delta Z = 0 \text{ for } i \neq 0)$.

5. Numerical examples

All the described excitations and loads have been included in a general large-domain (higher-order) integral-equation method for analysis of 3D electromagnetic structures composed of thin wires, metallic surfaces, and inhomogeneous dielectric bodies [7], and the associated General ElectroMagnetic code, GEM. Numerical results presented below were all obtained by GEM.

5.1. Metallic surface antenna

As the first example, consider half a bow-tie antenna above a ground plane, Fig. 5, driven at the base (at the ground plane) by a line-delta generator. The dimensions of the antenna are given in the figure caption. The conductance and susceptance of the antenna versus frequency are shown in Fig. 6. Also shown are experimental results [4] and those for the same antenna with a short cylindrical segment of diameter the same as the strip width (the segment is short, and there is no need for the equivalent diameter), driven by a TEM magnetic-current frill with $b/a = 2.3$. We see an excellent agreement between the three sets of results. Note that if the wire segment is used, a wire-to-plate junction model [4] is needed.

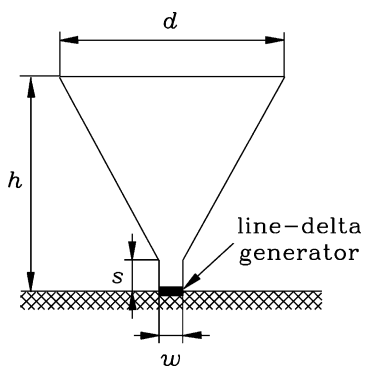

Fig. 5. Half a bow-tie antenna above ground plane ($w = 6$ mm, $d = 110$ mm, $h = 108$ mm, $s = 12$ mm).

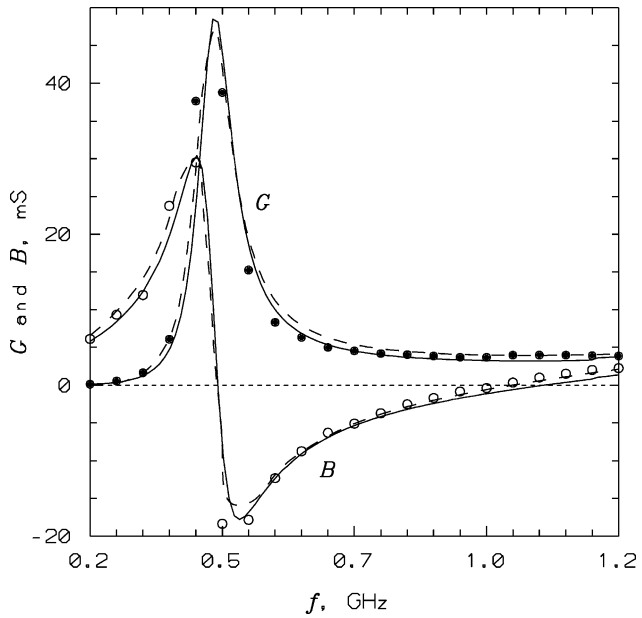

Fig. 6. Conductance (G) and susceptance (B) of the antenna from Fig. 5, versus frequency — line-delta generator, – – – TEM magnetic-current frill, ●, ○ measured [4].

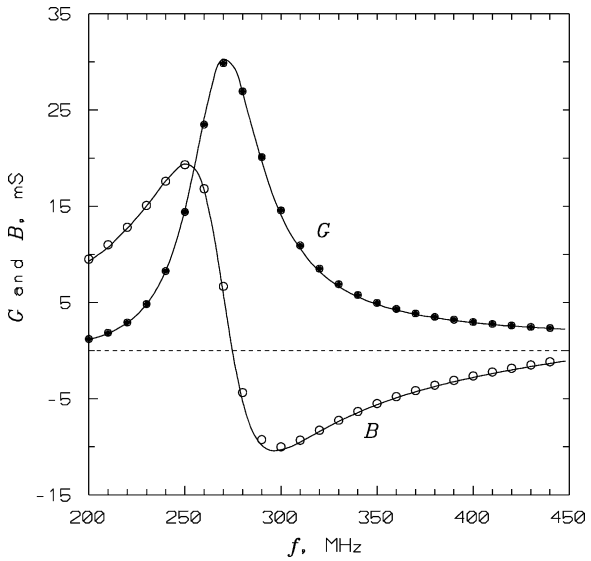

Fig. 8. Conductance (G) and susceptance (B) of the antenna from Fig. 7, versus frequency — line-delta generator, ●, ○ equivalent wire antenna with coaxial magnetic coating (results obtained with WireZeus [3]).

5.2. Printed strip antenna

Shown in Fig. 7 is a printed strip monopole antenna above a ground plane. The details are given in the figure caption. The antenna is considered with the finite dielectric substrate, as indicated. Fig. 8 shows the antenna conductance and susceptance versus frequency, compared with the results for the equivalent wire antenna with coaxial magnetic coating obtained with WireZeus [3] (this equivalency is possible for printed narrow-strip antennas on thin substrates). An excellent agreement of the two sets of results is observed.

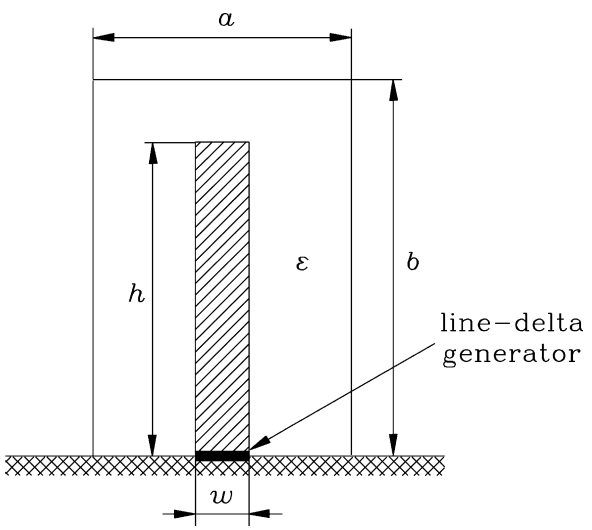

Fig. 7. Printed strip monopole antenna above ground plane ($h = 250$ mm, $w = 10$ mm, $a = 40$ mm, $b = 270$ mm, $\varepsilon_r = 2$, thickness of the substrate is $t = 2$ mm).

Note that if a model with a point-delta generator (or a TEM magnetic-current frill) is used, in conjunction with $\mathbf{J}_s$ and $\mathbf{D}$ as unknown quantities over the strip and in the dielectric substrate, respectively, a short wire segment is needed, which has to be partly immersed into the dielectric substrate. As a consequence, delicate partitioning of the part of the substrate which is in contact with the wire is required, resulting in less stable results.

5.3. Capacitively loaded strip antenna

The impedance and radiation pattern of thin cylindrical antennas can be made remarkably broadband by appropriate loads along their length [2]. Capacitive loads are easiest to manufacture, and do not introduce losses. We consider such a case as an example.

If there are only few loads separated by distances much greater than the wire radius, any technique for thin-wire analysis can predict the antenna properties accurately. If the loads are close, however, this is not possible due to the reduced kernel approximation. The proposed line-delta loads and generators enable a significantly more accurate analysis of such structures.

Consider the capacitively loaded strip monopole antenna sketched in Fig. 9. The dimensions of the strip segments are given in the figure caption. Let the capacitance between the strips be $C = 1.3$ pF, corresponding to a reactance of $X_C = -j122\ \Omega$ at 1 GHz. Shown in Fig. 10 is the conductance and susceptance of the antenna. We observe that the antenna exhibits a remarkable broadband property in its admittance.

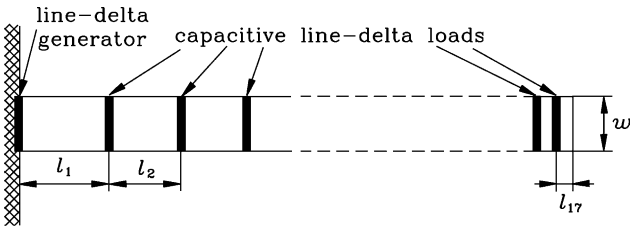

Fig. 9. Capacitively loaded strip monopole antenna. The strip width is $w = 0.84$ cm, and the segment lengths, $l_1, l_2, \ldots, l_{17}$, equal to (centimeters): 3.01, 2.97, 2.87, 2.65, 2.5, 2.2, 1.9, 1.7, 1.4, 1.1, 1.0, 0.8, 0.6, 0.5, 0.4, 0.3 and 0.24, respectively.

5.4. Imperfectly-conducting rod antenna

Consider next a simple example of a resistive rod of square cross-section, of cross-section area $S = 1$ cm^2, and of length $l = 50$ cm. Let the rod be made of a conductive material, of relative permittivity $\varepsilon_r = 1$ and conductivity $\sigma = 1$S/m. Assume that the rod is excited in the middle by a surface-delta generator of frequency $f = 300$ MHz, and emf $V = (1 + j0)V$. Due to large losses, such an antenna practically does not radiate (the antenna efficiency is only $\eta \simeq 1\%$).

The structure was analyzed in two ways: (1) as described, using the volume formulation of the Galerkin large-domain method (Section 4), and (2) as an equivalent wire dipole (Section 2), of radius $a = \sqrt{S/\pi}$ (the electrostatic equivalent radius of the square rod), with a constant resistance per unit length of $R' = 1/(\sigma S) = 10\ \Omega$/m. (For evaluating R' we can use the dc formula, since the skin effect is not pronounced-the skin depth is about 3 cm.)

Fig. 11 shows the current intensity, $I(u)$, along one half of the rod, obtained by the two procedures. The admittance as observed by the surface-delta generator is $Y_{\text{rod}} = (0.995 + j0.976)$ mS, while the admittance observed by the point-delta generator is $Y_{\text{wire}} = (1.06 + j1.04)$ mS. From Fig. 11 and from the admittance values we notice an excellent agreement of the two groups of

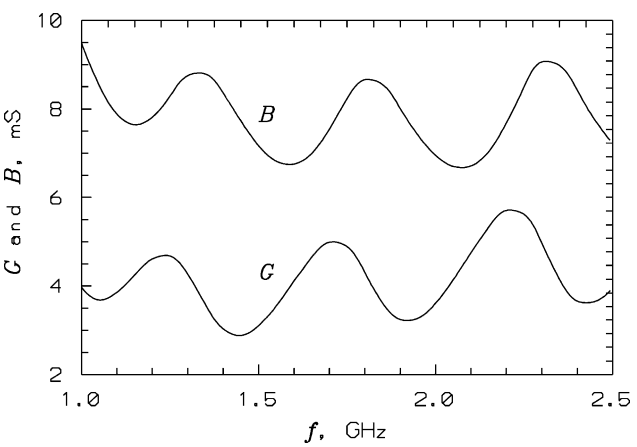

Fig. 10. Conductance (G) and susceptance (B) of the antenna from Fig. 9, versus frequency.

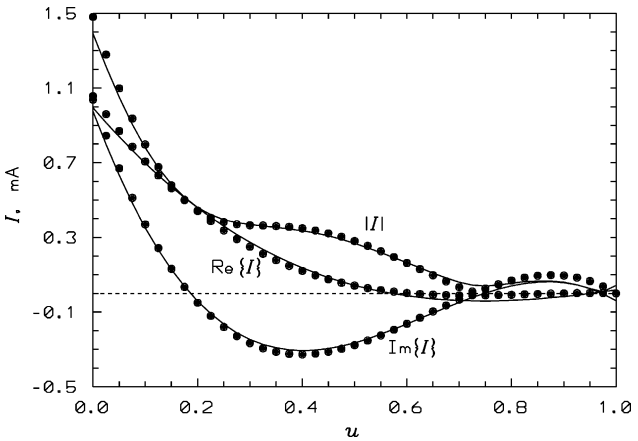

Fig. 11. Current intensity along one half of a resistive rod of square cross-section described in the text — surface-delta generator, volume formulation (Section 4) ● ● ● equivalent wire dipole (Section 2).

results, i.e. that the surface-delta generator yields the results of the same order of accuracy as the point-delta generator.

5.5. Conical dielectric antenna

As another example of the application of the surface-delta generator, consider the conical dielectric antenna of square cross-section shown in Fig. 12. We assume the antenna to be excited by the indicated surface-delta generator. Note that any other generator model (e.g. two plates pressed onto the small frustums and interconnected by a short piece of wire with a point-delta generator) would be both very complicated, and the results could be quite unstable. The excitation with the surface-delta generator is the simplest possible and yields very stable results. In addition, this kind of excitation is simple to realize using a section of a strip line.

Let the relative permittivity of the cone be $\varepsilon_r = 25$, the generator region be of side $a = 2$ cm, the large base of

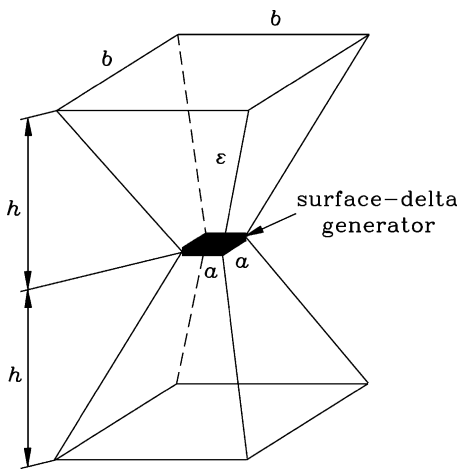

Fig. 12. Conical dielectric antenna of square cross-section.

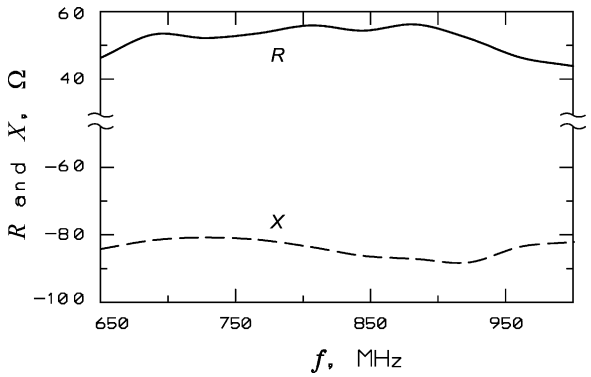

Fig. 13. Resistance (R) and reactance (X) of the antenna from Fig. 12, versus frequency.

the frustum be of side $b = 6$ cm, and its height be $h = 10$ cm. Such an antenna turns out to be remarkably broadband in both impedance and radiation pattern. The operating range of the antenna is between 650 MHz and 1 GHz. Fig. 13 shows the resistance and reactance of the antenna versus frequency. Note that with a compensating network for the antenna reactance, a VSWR can be obtained of less than 2 with respect to 50Ω in that frequency range.

6. Conclusions

This paper has summarized the models for excitations and loads commonly used in the analysis of 3D electromagnetic structures based on BEM (MoM), and has proposed simple new line-delta generators and loads and surface-delta generators and loads. The first type of generators and loads is extremely useful in the analysis of structures (antennas, circuits, and devices) consisting of conducting surfaces, and the other one in the analysis of structures containing dielectric bodies. Although simple physically, the models require considerable analytical preparations in order to be implemented in an actual algorithm. The paper has provided the complete derivations and expressions for the Galerkin generalized voltages and impedances corresponding to the new generators and loadings.

The usefulness of the proposed generator and load models is illustrated on a number of examples. On one side, the examples illustrate significant reduction in the complexity of the electromagnetic models with these new generators and loads, as compared with any generators and loads used so far. On the other side, the results obtained are stable and agree very favourably with available experimental and theoretical results.

It is believed that the novel simple models of generators and loads can be incorporated in other methods for the analysis of 3D electromagnetic systems, with comparable advantages as in the large-domain (higher-order) Galerkin BEM outlined in this paper.

References

[1] Harrington RF. Field computation by moment methods. New York: Macmillan; 1968.
[2] Popović BD, Dragović MD, Djordjević AR. Analysis and synthesis of wire antennas. Chichester/New York: Research Studies Press/Wiley; 1982.
[3] Popović BD. CAD of wire antennas and related radiating structures. Chichester/New York: Research Studies Press/Wiley; 1991.
[4] Popović BD, Kolundžija BM. Analysis of metallic antennas and scatterers. London: IEE Electromagnetic Wave Series, No. 38; 1994.
[5] Notaroš BM, Popović BD. General entire-domain method for analysis of dielectric scatterers. IEE Proc—Microwaves, Antennas Propagation 1996;143(6):498–504.
[6] Notaroš BM, Popović BD. General entire-domain Galerkin method for analysis of wire antennas in the presence of dielectric bodies. IEE Proc—Microwaves, Antennas Propagation 1998;145(1):13–18.
[7] Notaroš BM, Popović BD. Large-domain integral-equation method for analysis of general 3-D electromagnetic structures. IEE Proc—Microwaves, Antennas Propagation 1998;145(6):491–495.
[8] Volakis JL, Chatterjee A, Kempel LC. Finite element method for electro-magnetics. New York: IEEE Press; 1998.
[9] Popović BD. Electromagnetic field theorems. IEE Proc Part A 1981; 128(1):47–63.

Branislav M. Notaroš, born in 1965 in Zrenjanin, Yugoslavia, received the Dipl.Eng., MSc, and PhD degrees in electrical engineering from the University of Belgrade, Yugoslavia, in 1988, 1992, and 1995, respectively. He is currently an Assistant Professor of Electrical and Computer Engineering at the University of Massachusetts Dartmouth, USA. From 1996 to 1998, he was an Assistant Professor in the Electrical Engineering Department at the University of Belgrade. He spent the 1998–1999 academic year as a Research Associate at the University of Colorado at Boulder. Prof. Notaroš research interests are predominantly in computational electromagnetics and in antenna design. His publications include 10 journal papers, 32 conference papers, a book chapter, and three university workbooks. He is the Director of the Telecommunications Laboratory in the Advanced Technology and Manufacturing Center at UMass Dartmouth. Dr Notaroš was the recipient of the 1999 Institution of Electrical Engineers (IEE) Marconi Premium.

Branko D. Popović has been a Professor of Electrical Engineering at the University of Belgrade, Yugoslavia, for four decades. He was a Visiting Professor at the Virginia Polytechnical Institute, University of Colorado, McGill University, and Chengdu University. In 1999, he was with the wireless company Celletre Ltd, Haifa, Israel. He has authored or co-authored numerous papers on antennas and applied electromagnetics, six textbooks in fundamentals of electrical engineering and electromagnetics, three monographs on the analysis and computer-aided design (CAD) of wire and metallic antennas and scatterers, and two program packages. Dr Popović is a member of the Serbian Academy of Sciences and Arts and is a Fellow of the Institution of Electrical Engineers (IEE), UK. He was the recipient of the 1974 Institution of Electronics and Radio Engineers (IERE) Heinrich Hertz Premium, the 1985 IEE James Clerk Maxwell Premium, the 1985 Yugoslav Nikola Tesla Premium, the 1999 IEE Marconi Premium, and numerous Yugoslav awards.